ELSEVIER

Nuclear Instruments and Methods in Physics Research B 180 (2001) 23–31

NIM B
Beam Interactions with Materials & Atoms

www.elsevier.nl/locate/nimb

Mechanical property degradation in irradiated materials: A multiscale modeling approach

B.D. Wirth [a,*], M.J. Caturla [a], T. Diaz de la Rubia [a], T. Khraishi [b], H. Zbib [b]

[a] *Lawrence Livermore National Laboratory, Chemistry and Materials Science Dir., P.O. Box 808, L-353 Livermore, CA 94550, USA*
[b] *Washington State University, Pullman,WA, USA*

Abstract

High-energy particle irradiation of low stacking fault energy, face centered cubic (fcc) metals produces significant degradation of mechanical properties, as evidenced in tensile tests performed at or near room temperature. Post-irradiation microstructural examination reveals that approximately 90% of the radiation-induced defects in copper are stacking fault tetrahedra (SFT). Radiation damage is an inherently multiscale phenomenon involving processes spanning a wide range of length and time scales. Here we present a multiscale modeling methodology to study the formation and evolution of defect microstructure and the corresponding mechanical property changes under irradiation. At the atomic scale, molecular dynamics (MD) simulations have been used to study the evolution of high energy displacement cascades, SFT formation from vacancy rich regions of displacement cascades, and the interaction of SFTs with moving dislocations. Defect accumulation under irradiation is modeled over diffusional length and time scales by kinetic Monte Carlo (KMC), utilizing a database of displacement cascades generated by MD. The mechanical property changes of the irradiated material are modeled using three-dimensional dislocation dynamics (DD). Key input into the DD includes the spatial distribution of defects produced under irradiation, obtained from KMC, and the fate of dislocation interactions with SFTs, obtained from MD.

1. Introduction

The effect of irradiation on materials microstructure and properties is an inherently multiscale phenomenon, involving processes spanning a wide range of length and time scales. At the smallest scales (nanometer and picosecond), high-energy particles collide with lattice atoms and the resulting displacement collision cascades produce highly non-equilibrium point defect and point defect cluster concentrations with a high degree of spatial correlation. The defects cluster and diffuse over macroscopic length and time scales, significantly altering the materials chemistry and microstructure. Changes in microstructure are responsible for dimensional instabilities, such as swelling and irradiation creep [1–3], and mechanical property changes and degradation [1,4,5], such as irradiation hardening and changes in the post-yield deformation behavior including plastic flow localization [5], which impact component performance, reliability and ultimately, lifetime.

* Corresponding author. Tel.: +1-925-424-9822; fax: +1-925-423-7040.
E-mail address: wirth4@llnl.gov (B.D. Wirth).

0168-583X/01/$ - see front matter
PII: S0168-583X(01)00392-5

In metals, decades of research have demonstrated the significant degradation of mechanical properties that result from exposure to high-energy particle irradiation. The key features of radiation damage on mechanical behavior are illustrated in Fig. 1 [4,5] and can be summarized as:

1. at low to intermediate dose, a sharp increase in yield stress followed by a generally reduced strain hardening capacity and reduced ductility to failure;
2. at higher doses, the appearance of a yield point followed by a yield drop; and perhaps most interestingly;
3. an instability that results in plastic flow localization and leads to further loss of ductility and premature failure.

Such changes in mechanical properties result from corresponding changes in the material microstructure [4]. Thus, the key to understanding and predicting mechanical property changes during irradiation relies on having a detailed understanding of both the materials microstructure as it evolves during irradiation and the link between microstructure and mechanical properties.

Recent years have witnessed rapid advances in computational capabilities for the realistic simulation of complex physical phenomena, such as irradiation and aging effects. And, substantial advances have been made in understanding the effects of irradiation in pure metals, such as iron, copper and palladium [5–7]. In this paper, we present some of our preliminary work in this field, which illustrates a complete multiscale application of predicting microstructural evolution and mechanical property changes during irradiation for the case of pure metals.

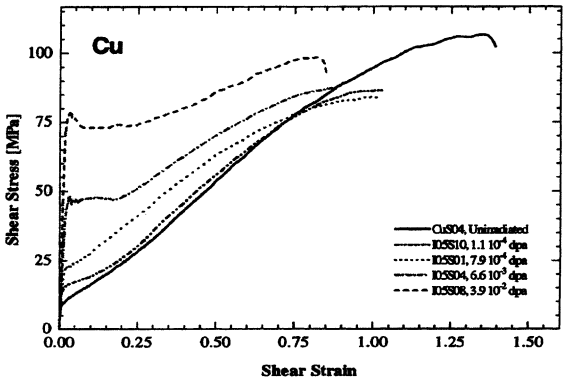

Fig. 1. Stress–strain behavior of single crystal Cu as a function of irradiation dose from 1.1×10^{-4} to 3.9×10^{-2} dpa [5].

2. Multiscale modeling methodology

The modeling methodology involves a hierarchical approach integrating ab initio electronic structure calculations, MD simulations and KMC over the relevant length and time scales to model the fates of defects and solutes and thus, predict microstructural evolution during irradiation in metals. The prediction of material microstructure is linked to a quantitative prediction of irradiation hardening and post-yield deformation behavior through the use of three-dimensional DD simulations.

Specifically, the multiscale modeling approach, schematically illustrated in Fig. 2, relies on the following elements:

1. *Ab initio electronic structure calculations*. Basic defect properties (formation, binding and migration energies of point defects and small point defect clusters including the interaction with solutes) can be obtained from ab inito methods involving plane wave pseudopotential codes using the generalized gradient (GGA) and local density (LDA) approximations [8]. The electronic structure calculations of interatomic forces, interactions and energetics provide key parameters for KMC models and are instrumental in the development and fitting of semi-empirical, embedded atom method (EAM) alloy potentials.
2. *Molecular dynamics*. Defect properties of larger defects can be obtained from atomistic simulations based on semi-empirical EAM potentials containing up to 100 million atoms for times approaching 100 ns. In addition to defect cluster energetics, MD simulations of displacement cascade evolution provide a database of primary damage production, and large-scale simulations can provide physical insight into kinetic processes and interactions, including the fate of moving dislocations as they interact with dislo-

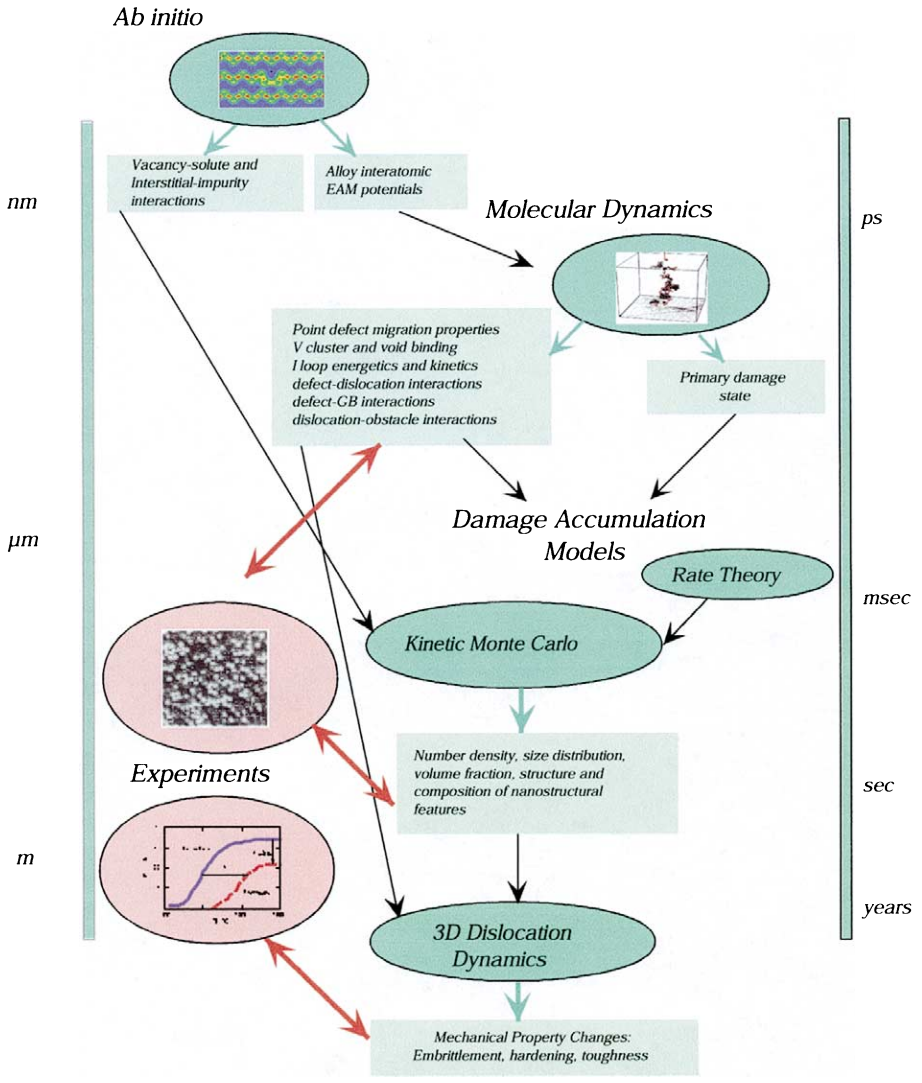

Fig. 2. Multiscale modeling approach illustrating the integration of length and time-scales accomplished through modeling predictions (light grey arrows), the linking of different modeling techniques (black arrows) and the use of experimental validation (red arrows).

cation loops, defect clusters and second phase particles.

3. *Linkage to kinetic Monte Carlo*. The spatial correlations of defects produced within a cascade are introduced into a KMC simulation, at the appropriate displacement rate, from a MD database and superimposed on the initial microstructure and dislocation densities. Defect migration and binding energetics, derived from ab initio and MD methods as well as experiment also serve as input to KMC models.
4. *Kinetic Monte Carlo*. Defect and solute diffusion, interactions, clustering and second phase formation occur over seconds and microns and are inaccessible to MD and must be modeled using either rate theory or KMC. Both methods solve kinetic reaction-diffusion equations. However, rate theory solves the equations

in a one-dimensional space containing no spatial information, while KMC solves the equations in fully three-dimensional space and thus captures all of the inherent spatial correlation and fluctuations. For this reason, we use KMC to track the fates of all defect species and provide a prediction of the microstructural evolution under irradiation. Specifically, this includes the number, size and spatial distribution of the dislocation loops, self-interstitial, vacancy and defect-solute clusters.

5. *Linkage to mechanical property changes*. Mechanical properties of a material depend on the underlying microstructure. The microstructure predicted by KMC simulation serves as input to three-dimensional DD simulation to quantitatively predict radiation-induced mechanical property changes.
6. *Three-dimensional dislocation dynamics*. The collective behavior of an ensemble of dislocations in a crystal, which can be hundreds of microns in size, is modeled by calculating the forces on each dislocation and taking into account all possible reactions among dislocations, as well as between network dislocations, and the radiation-induced defect microstructure [9–11]. A key component to quantitative DD simulations is understanding the mechanisms and fates of a variety of nanostructural features which interact with moving dislocations, obtained from dislocation theory and large-scale MD simulations.

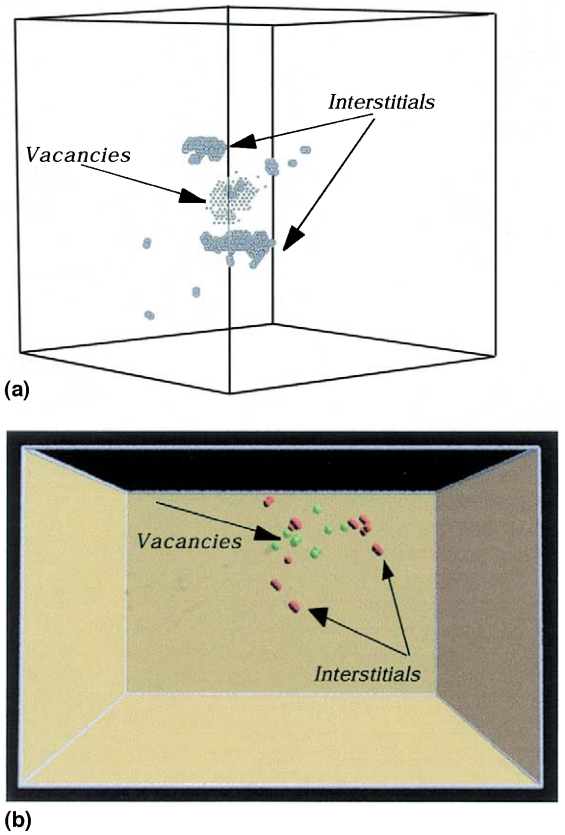

Fig. 3. Primary damage produced in a 20 keV displacement in (a) Cu and (b) W. In Cu, large self-interstitial clusters are formed on the cascade periphery and substantial vacancy clustering to a planar loop occurs within the cascade core. In W, a number of very small self-interstitial clusters form on the cascade periphery, while little or no vacancy clustering occurs within the cascade core.

3. Primary damage production and microstructural evolution

The physics of primary defect production in high-energy displacement cascades has been extensively studied by a number of groups using molecular dynamics simulations [12–14]. Displacement cascades result from the collision of high energy particles (e.g., neutron, alpha, proton or heavy ion) with lattice atoms and, in most metals, evolve over a few tens of picoseconds to produce a spatially correlated distribution of vacancies, self-interstitials and their clusters. Fig. 3 shows an example of the primary damage produced in fcc copper and bcc tungsten by a 20 keV displacement cascade. In fcc metals, large vacancy and self-interstitial clusters are produced within a few tens of picoseconds as the kinetic energy is dissipated and the cascade cools. In bcc metals, cascade evolution is generally similar, however, the resulting self-interstitial clusters are smaller and no significant vacancy clustering occurs during the cascade (10 ps) time scale [12–14].

MD [12–19] and KMC [6,20,21] simulations have been instrumental in understanding both the structure and migration properties and subsequent evolution of the vacancy and self-interstitial clus-

ters formed in fcc and bcc metals. A comparison between the damage accumulation in Cu and Fe has been recently performed by Caturla et al. [6]; in this paper, we will briefly review the key aspects of microstructure evolution in Cu and then demonstrate a method for linking the changes in microstructure to mechanical properties.

In low stacking fault energy fcc metals, such as Cu, the clustered vacancies produced in the displacement cascade (Fig. 3(a)) collapse to form SFT within a few picoseconds at room temperature [15]. SFT formation occurs by a dislocation mechanism, consistent with that first proposed by Silcox and Hirsch [22], and discussed in more detail by Wirth et al. [15]. Interestingly, the MD simulations predict that the SFT structure will not consist of perfect tetrahedron, but in most cases, will actually consist of truncated tetrahedron [15,16] and even some overlapping, truncated SFT [1] [15].

The character and migration properties of self-interstitial clusters have also been extensively studied by MD simulation. The results, in both fcc and bcc metals, show that prismatic (glissile) self-interstitial clusters are formed in the cascades and MD simulations have shown that the clusters migrate one-dimensionally with very low activation energies [17–19]. Osetsky et al. [19] have performed the most extensive simulations in Cu, characterizing cluster diffusivity as a function of size and, showing that cluster mobility is significantly reduced for cluster sizes above about 100.

Information about the character and energetics of the vacancy and self-interstitial clusters, along with an MD database of the spatial distribution of primary damage production can be used in a KMC model of damage accumulation. The details of the KMC code are described in more detail elsewhere [6]; but briefly, KMC tracks the location, diffusion and reactions of defects, impurities and clusters as a function of time. The starting point in these simulations is the primary damage state, i.e., the spatially correlated locations of vacancy and interstitials, obtained from MD simulations of displacement cascades, and the appropriate activation energies for diffusion and dissociation, as well as the reactions that occur between species. The defects execute random diffusion jumps (in one, two or three dimensions depending on the nature of the defect) with a probability proportional to their diffusivity. Similarly, cluster dissociation rates are governed by a dissociation probability that is proportional to the binding energy of a particle to the cluster.

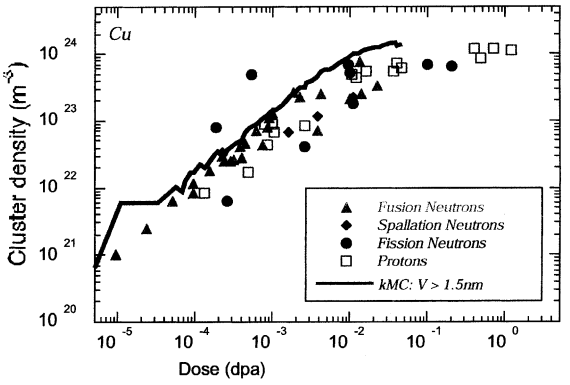

Fig. 4. Evolution of the visible cluster defect density as a function of dose. The KMC predictions, shown by the solid line, are compared to a collection of experimental data from [23].

Fig. 4 shows a comparison between a number of experimental results [23,24] and KMC predictions of the visible [2] defect accumulation in Cu, when neutron irradiated near room temperature. Both the visible defect density (Fig. 4) and the KMC prediction that over 90% of the visible point defect clusters in irradiated Cu are vacancy SFT are in excellent agreement with experiments [23,24]. Further, the KMC results predict a constant mean SFT size with increasing irradiation,

[1] A triangular vacancy platelet on a $\{1\,1\,1\}$ plane bounded by three $\langle 1\,1\,0\rangle$ directions forms a single SFT. A triangular vacancy platelet bounded by two $\langle 1\,1\,0\rangle$ and one $\langle 1\,1\,2\rangle$ directions forms two partial (truncated) SFTs, one above and one below the initial plane; we define this as an overlapping truncated SFT.

[2] Transmission electron microscopy studies quote values between 1.5 and 2 nm as the minimum defect size resolvable in the microscope [23,24]. We have used $L = 1.5$ nm for SFT and $d = 2$ nm for self-interstitial dislocation loops, along with simple geometric relations to estimate the minimum number of defects in a visible cluster as $N = 20$ and 55 for vacancies (SFT) and self-interstitials (loops), respectively [6].

once again in good agreement with experimental observations [23,24]. The spatial distribution, size and type of clusters formed during irradiation can be mapped into a dislocation dynamics simulation to study the evolution of the underlying dislocation structure under applied stress to provide a quantitative prediction of the mechanical property behavior (e.g., a stress–strain curve).

4. Linking microstructure to mechanical properties

The strength and flow properties of a metal depend on the underlying microstructure and the ease with which dislocations move through the material. DD simulates a material stress–strain curve by following the motion and interaction of an ensemble of dislocations in a small, three-dimensional crystal, as it evolves with time [9–11]. In our DD simulations [7,9–11], the dislocations are discretized in straight-line segments that move under the action of an applied stress, including the stress field of all surrounding dislocations. Dislocation multiplication can occur by a variety of mechanisms that may involve superjog collisions [25], standard Frank–Read (FR) sources and double cross slip [7]. Further, dislocation segments interact with the irradiation-induced defect clusters. The mechanism and fates of these interactions are obtained from large-scale MD simulations, as well as dislocation theory.

We have successfully coupled the results of atomistic predictions of microstructure evolution to three-dimensional mesoscale DD simulation to investigate the corresponding mechanical behavior in irradiated Cu and Pd [7]; here we provide a brief example for the case of Cu. The DD simulation is performed in a 10 μm cube containing an initial density of FR dislocation sources distributed at random on $\{1\,1\,1\}$ planes, the primary slip planes in fcc metals. Reflection boundary conditions are applied, as described by Zbib et al. [9]. The spatial distributions of defects obtained from multiscale simulations of irradiation induced microstructural evolution are mapped into the DD cell. The distributions contain bulk sessile (SFT and loops) defect clusters, and following the cascade-induced source hardening model [27,28], defect clusters which decorate the FR sources along the dislocation line. [3]

The elastic interaction between a moving dislocation and a defect cluster (loop or SFT) can be obtained from dislocation theory; however, details regarding the fate of such interactions must come from large-scale MD simulations. To address this point, we have initiated MD studies to catalog the matrix of possible dislocation–SFT interactions. Fig. 5 shows the results of one such simulation involving 955,155 atoms at 100 K in Cu. In this simulation, an overlapping, truncated SFT [1], such as formed by aging displacement cascades [15], with a spacing of 14 nm (along the dislocation line) is placed on the glide plane of a dissociated edge dislocation which moves under an applied shear stress (300 MPa). [4] Fig. 5(a) shows the initial configuration of the edge dislocation, split into two Shockley partial dislocations, and the overlapping, truncated SFT (most easily visualized in $\langle 1\,1\,0\rangle$ projection), as represented through visualization of the atoms with high potential energy. Fig. 5(b) shows that upon contact, the leading partial is pinned, absorbs part of the overlapping SFT and climbs as the trailing partial approaches. Fig. 5(c) shows that the trailing partial catches the leading partial at the location of the overlapping SFT, constricts and climbs with absorption of the remaining defect, which results in the formation of a pair of superjogs. Following defect absorption, the dislocation continues to move (Fig. 5(d)), but with a decreased mobility associated with superjog pinning.

[3] The initial position of the defect clusters which decorate dislocations is chosen such that (i) the distance between the defect cluster and the dislocation is slightly larger than the stand-off or absorption distance [27,28] and (ii) the location results in a negative (attractive) dislocation–defect interaction energy [29].

[4] It is important to provide some details regarding this simulation. First, the EAM potential used for Cu gives a stacking fault energy of 11.4 mJ/m^2, which is lower than experiment values (30–40 mJ/m^2) and results in a large separation between the two Shockley partials. Second, the applied stress (300 MPa) is significantly higher than the yield stress of copper and was used to study the fate of the interaction within readily accessible MD simulation times. Additional simulations are ongoing to characterize the effect of these (and other) variables on the results.

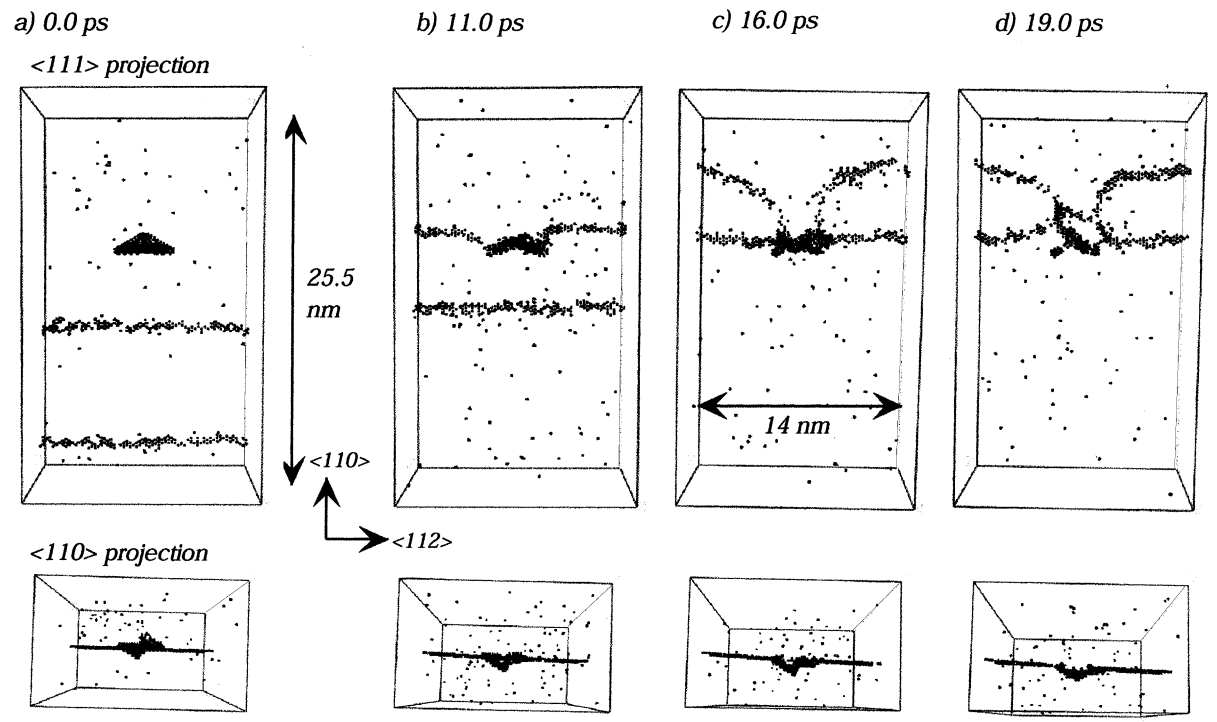

Fig. 5. Molecular dynamics simulation of the interaction between a dissociated edge dislocation and an overlapping, truncated SFT [1] in Cu. The high potential energy atoms are visualized in $\langle 1\,1\,1\rangle$ (top) and $\langle 1\,1\,0\rangle$ (bottom) projections and show the motion of the two Shockley partials and interaction with the overlapping, truncated SFT at (a) 0, (b) 11.0, (c) 16.0 and (d) 19.0 ps after application of a 300 MPa shear stress. See text for additional details.

The detailed absorption mechanism is complicated and has not yet been completely analyzed. However, it is clear that defect absorption by the dislocation produces climb and the formation of superjog pairs. One of the superjogs is initially constricted, presumably in the form of a Lomer segment, as discussed by Rodney and Martin [30] for the case of climb associated with self-interstitial cluster absorption. The constricted superjog has a decreased mobility, but can transform to a more favorably configuration through the incorporation of three self-interstitials, as discussed in [30]. This process occurred just prior to the snapshot shown in Fig. 5(c), and indeed, the small cluster of high energy atoms seen below the left superjog in Fig. 5(d) has been identified to consist of three vacancies. Additional simulations are underway to characterize the matrix of possible dislocation-SFT interactions, including the effect of applied stress and stacking fault energy, and provide rules for DD simulations that can provide insight into the mechanisms responsible for flow localization in irradiated metals.

An example of the application of DD to predicting the strengthening and flow properties of irradiated metals is shown in Fig. 6. The figure shows the stress–strain curves obtained with our DD simulations for Cu, considering the elastic interactions between the defects and dislocations. The DD simulation was performed with an initial dislocation density of $\rho_N = 10^{12}$ m^{-2} and without irradiation defects, the system yields at around 37 MPa. Defects were introduced into the DD box, both in the bulk and decorating the dislocations, to account for the irradiation-induced defect field. Following the introduction of a bulk defect density, $\rho_B = 8.4 \times 10^{21}$ m^{-3}, which corresponds to an average SFT spacing of ≈ 50 nm, two behaviors are seen. When the defect density along the line (ρ_D) is very high, i.e. $\rho_D \gg \rho_B$ and the average

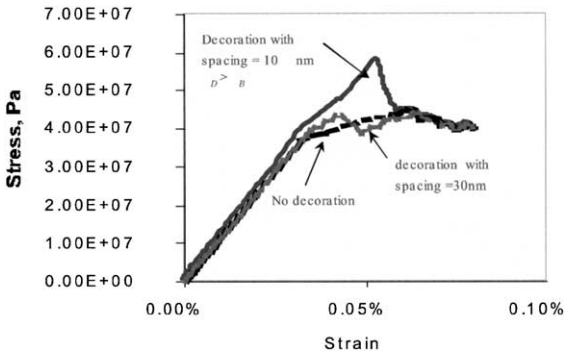

Fig. 6. Dislocation dynamics results of stress–strain curves showing the effect of radiation produced defect spacing (decoration) along the dislocation line. See text for additional details.

spacing along the line is only 10 nm, a clear yield point followed by a yield drop can be observed. The appearance of the yield point can be attributed to the cluster-induced source hardening mechanism proposed by Singh et al. [26,27]. However, when the average spacing between defects along the dislocation line is 30 nm, which is comparable to that in the bulk, the system yields at a slightly higher stress and only a very diffuse yield drop is apparent. This is in excellent agreement with experiment [5] which shows that the observed yield drop disappears at elevated doses where $\rho_D \approx \rho_B$.

5. Summary

We have presented a multiscale modeling methodology to study mechanical property changes under irradiation. The modeling methodology is based upon atomistic simulations to provide the primary defect production in displacement cascades and key defect properties and KMC simulations to model damage accumulation and microstructural evolution under irradiation. The link between microstructure and mechanical properties is performed using three-dimensional dislocation dynamics. We presented selected results from a study of the microstructural evolution and mechanical property changes in Cu, which are in good agreement with experiments. Future work will focus on the continued improvement of simulation methods and the extension to treating irradiation and aging effects in more complex, multicomponent alloy systems.

Acknowledgements

This work was performed under the auspices of the U.S. Department of Energy by University of California Lawrence Livermore National Laboratory under contract No. W-7405-Eng-48.

References

[1] L.K. Mansur, E.E. Bloom, J. Met. 34 (1982) 23.
[2] L.K. Mansur, J. Nucl. Mater. 216 (1994) 97.
[3] F.A. Garner, J. Nucl. Mater. 205 (1993) 98.
[4] G.E. Lucas, J. Nucl. Mater. 206 (1993) 287.
[5] M. Victoria, N. Baluc, C. Bailat, Y. Dai, M.I. Luppo, R. Schaublin, B.N. Singh, J. Nucl. Mater. 276 (2000) 114.
[6] M.J. Caturla, N. Soneda, E.A. Alonso, B.D. Wirth, T. Diaz de la Rubia, J. Nucl. Mater. 276 (2000) 13.
[7] T. Diaz de la Rubia, H.M. Zbib, T.A. Khraishi, B.D. Wirth, M. Victoria, M.J. Caturla, Nature 406 (2000) 871.
[8] G. Kresse, J. Hafner, Phys. Rev. B 47 (1993) 558.
[9] H.M. Zbib, M. Rhee, J.P. Hirth, Int. J. Mech. Sci. 40 (1998) 113.
[10] M. Rhee, H.M. Zbib, J.P. Hirth, H. Huang, T. Diaz de la Rubia, Modeling Simul. Mater. Sci. Eng . 6 (1998) 467.
[11] H.M. Zbib, T. Diaz de la Rubia, M. Rhee, J.P. Hirth, J. Nucl. Mater. 276 (2000) 154.
[12] W.J. Phythian, R.E. Stoller, A.J.E. Foreman, A.F. Calder, D.J. Bacon, J. Nucl. Mater. 223 (1995) 245.
[13] R.E. Stoller, G.R. Odette, B.D. Wirth, J. Nucl. Mater. 251 (1997) 49.
[14] R.S. Averback, T. Diaz de la Rubia, Solid State Phys. 51 (1998) 281.
[15] B.D. Wirth, V. Bulatov, T. Diaz de la Rubia, J. Nucl. Mater. 283–287 (2000) 773.
[16] Yu.N. Osetsky, D.J. Bacon, Nucl. Instr. and Meth. B 180 (2001) 85.
[17] N. Soneda, T. Diaz de la Rubia, Philos. Mag. A 78 (1998) 995.
[18] B.D. Wirth, G.R. Odette, D. Maroudas, G.E. Lucas, J. Nucl. Mater. 276 (2000) 33.
[19] Y.N. Osetsky, D.J. Bacon, A. Serra, B.N. Singh, S.I.Y. Golubov, J. Nucl. Mater. 276 (2000) 65.
[20] D.G. Doran, Irradiat. Effects 2 (1970) 249.
[21] H.L. Heinisch, B.N. Singh, J. Nucl. Mater. 251 (1997) 77.
[22] J. Silcox, P.B. Hirsch, Philos. Mag. 4 (1959) 72.
[23] Y. Dai, M. Victoria, MRS Symp. Proc. 439 (1997) 319.
[24] B.N. Singh, S.J. Zinkle, J. Nucl. Mater. 206 (1993) 212.

[25] M. Rhee, D.H. Lassila, V.V. Bulatov, L. Hsuing, T. Diaz de la Rubia, Phil. Mag. Lett. (2001) submitted.
[26] B.N. Singh, A.J.E. Foreman, H. Trinkaus, J. Nucl. Mater. 249 (1997) 103.
[27] H. Trinkaus, B.N. Singh, A.J.E. Foreman, J. Nucl. Mater. 251 (1997) 172.
[28] N.M. Ghoneim, B.N. Singh, L.Z. Sun, T. Diaz de la Rubia, J. Nucl. Mater. 276 (2000) 166.
[29] T.A. Khraishi, H.M. Zbib, T. Diaz de la Rubia, Metall. Mater. Trans. B (2001) submitted.
[30] D. Rodney, G. Martin, Phys. Rev. B 61 (2000) 8714.